ACS NANOSCIENCE Au
AN OPEN ACCESS JOURNAL OF THE AMERICAN CHEMICAL SOCIETY

pubs.acs.org/nanoau
Article

Anodic Electrodeposition of IrO_x Nanoparticles from Aqueous Nanodroplets

Saptarshi Paul,[†] Joshua Reyes-Morales,[†] Kingshuk Roy, and Jeffrey E. Dick*

Cite This: *ACS Nanosci. Au* 2024, 4, 216−222
Read Online

ACCESS | Metrics & More | Article Recommendations | Supporting Information

ABSTRACT: Electrodeposition has been used for centuries to create new materials. However, synthetic platforms are still necessary to enrich a variety of nanomaterials that can be electrodeposited. For instance, IrO_x is a popular material for the water oxidation reaction, but electrodeposition strategies for the controlled growth of IrO_x nanoparticles are lacking. Here, we demonstrate the anodic electrodeposition of IrO_x nanoparticles from aqueous nanodroplets. Field emission scanning electron microscopy (FESEM) and scanning transmission electron microscopy (STEM) images confirm the macro- and microstructure of the resulting nanoparticles. IrO_x nanoparticles of 43 ± 10 nm in diameter were achieved. X-ray photoelectron spectroscopy (XPS) showed the presence of Ir(III) and Ir(IV) hydrated oxyhydroxide species. The synthesis of IrO_x nanoparticles under anodic conditions using water nanodroplets expands the capabilities of our technique and provides a tunable platform for IrO_x nanoparticle electrodeposition.

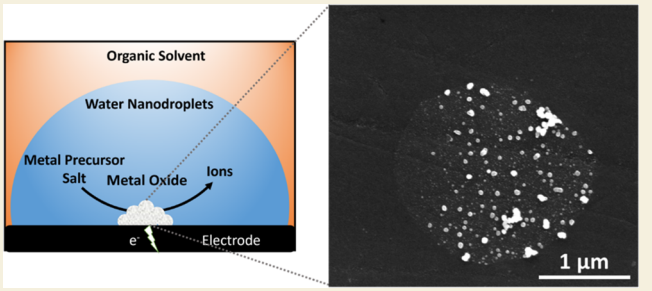

KEYWORDS: *nanodroplet-mediated electrodeposition, anodic electrodeposition, iridium oxide, nanoparticles, water nanodroplets*

INTRODUCTION

Electrodeposition as a tool for the synthesis of nanoparticles has been used extensively. The technique is versatile in that it can be used to synthesize metals,[1−6] metal oxides,[7−10] and alloys,[11−13] and it produces nanoparticles with high purity and homogeneity, which is crucial in its application in heterogeneous catalysis.[14−16] Electrodeposition has also been shown to be a scalable and cost-effective synthetic tool.[17−19] Various methods have been employed previously to synthesize IrO_x. Thermal decomposition can synthesize high-purity IrO_x, but the requirement of high temperature may cause aggregation of particles.[20] Sol−gel processes may produce uniform coatings of IrO_x, but may be quite time-consuming.[21] And IrO_x can also be prepared by bulk electrochemical deposition methods, which can be cost-effective and may be performed in aqueous solutions. Unfortunately, bulk electrodeposition suffers from many limitations, such as the inability to control the nanoparticle size, morphology, and microstructure.[22,23]

Our group has recently introduced nanodroplet-mediated electrodeposition for the controlled synthesis of nanoparticles with tunable size, shape, and composition.[24−30] In this method, nanoscale (~100 s of nanometers) droplets of a precursor solution containing the desired metal ions are generated and then deposited onto a conductive substrate. To date, only cathodic electrodeposition has been achieved. In these experiments, the voltage is biased negative enough to reduce the metal to the zerovalent metal. Amorphous materials (metallic glass high entropy alloy nanoparticles and cobalt oxyhydroxides) have been achieved by our group and Ahn's group independently.[31−33] However, such materials were deposited cathodically and likely follow an electroprecipitation reaction, where the water droplet is reduced by itself, creating an alkaline environment to precipitate out oxyhydroxides. In all cases, the composition, size, microstructure (amorphous versus crystalline), and morphology of the resulting nanoparticles are determined by the precursor solution composition, deposition conditions, etc.[24,30,34]

Nanodroplet-mediated electrodeposition has emerged as a promising technique for the controlled synthesis of nanoparticles with tailored properties. Its advantages include size and shape control, composition control, scalability, versatility, and cost-effectiveness.[24,26,28] These make it highly attractive for various applications, including electronics, catalysis, energy storage, and biomedical devices.

We report the first anodic electrodeposition of metal oxide nanoparticles from water nanodroplets. Our goal was to generate IrO_x nanoparticles as they exhibit high catalytic activity,[35,36] excellent electrical conductivity,[37] and stability,[38]

Received: November 30, 2023
Revised: February 6, 2024
Accepted: February 15, 2024
Published: April 18, 2024

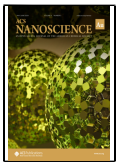

Scheme 1. Representative Figure of the Electrochemical Electrodeposition of IrO_x by Using Nanodroplet-Mediated Electrodeposition[a]

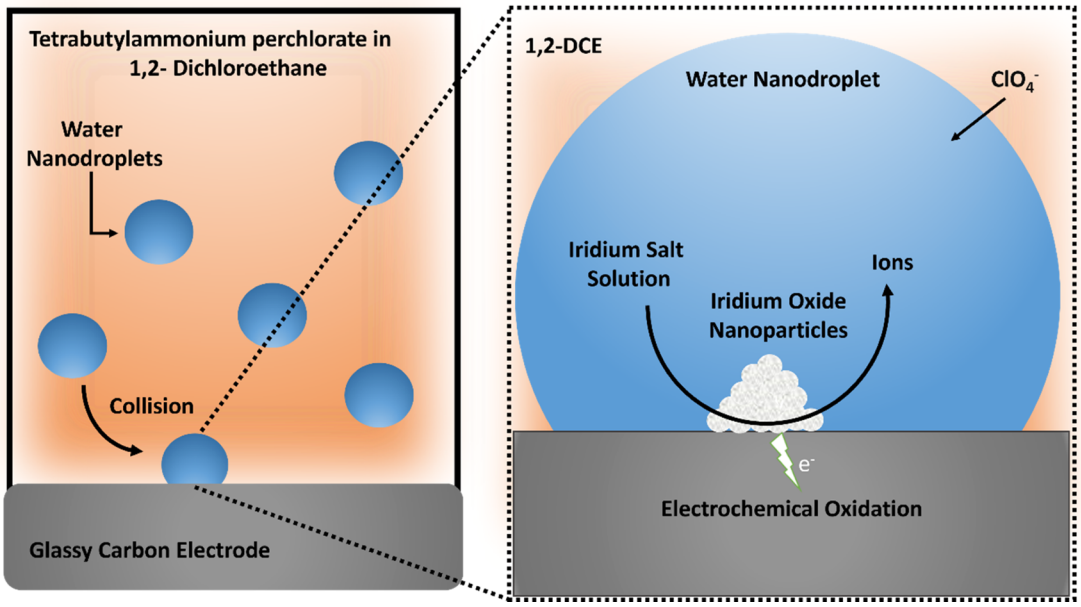

[a]Nanodroplets collide stochastically with the glassy carbon electrode surface. Since a positive potential is applied, the K_3IrCl_6 solution will be oxidized to generate IrO_x nanoparticles at the electrode−water interface.

making them particularly useful in energy storage devices,[39,40] sensing applications,[41] and also in biomedical applications.[42]

METHODOLOGY

Chemicals and Reagents

Chemicals such as potassium hexachloroiridate(III) (Sigma-Aldrich), tetrabutylammonium perchlorate, sodium hydroxide (≥98%), and 1,2-dichloroethane (99.8%) were purchased from Sigma-Aldrich. Potassium chloride was purchased from Fisher Scientist. Span 80 was purchased from TCI Chemicals and was used as received. A 3 mm glassy carbon macroelectrode as a working electrode and a Ag/AgCl reference electrode were purchased from CH Instruments, Austin, Texas. The reference electrode was stored in a solution of 1 M KCl. Additionally, a salt bridge made of 1 M KCl with 3% agarose was used for these experiments. The counter electrode was a glassy carbon rod. A fluorinated ethylene propylene tube was purchased from Oak Rids Centrifuge Tube from Thermo Scientific. This tube was used to prepare the emulsion solutions. Nanopure water (18.2 MΩ·cm) was used to prepare all of the aqueous-based solutions. A carbon type B 200 mesh Ni TEM grid was obtained from Ted Pella, Inc.

Instruments

A Q500 ultrasonic processor of 500 W (Qsonica, Newtown, CT) with a microtip probe was used to prepare the emulsion solutions. The applied parameters were an amplitude of 40% with a turn on and off for 5 s each for a total of 1 min. For the electrochemical experiments, a CHI model 601D potentiostat (CH Instruments, Austin, TX) was used. During this paper, all of the electrochemical data will be presented in polarographic notation (Texas). The electrochemical technique used to electrodeposit the nanoparticles was chronoamperometry. For electrochemical characterization, cyclic voltammetry (CV) was performed. Dynamic light scattering (DLS) was used to obtain the average size of the water droplets suspended in 1,2-dichloroethane. It used a Zetasizer Nano ZS instrument (Malvern, Westborough, MA). A Thermo Scientific Themis Z Double Aberration Corrected S/TEM was used to obtain the transmission electron microscopy (TEM) images of the IrO_x nanoparticles. To characterize the nanoparticle structure and elemental analysis, FEI Nova Nano SEM field-emission scanning electron microscopy (SEM) and energy-dispersive X-ray (EDX) were used. The voltage used during SEM and EDX were 10 and 20 kV, respectively.

Experimental Procedures

Different solutions were prepared for the electrodeposition process. In general, an aqueous solution containing 6 mM potassium hexachloroiridate(III), 20 mM KCl, and 55 mM NaOH in water was prepared. This aqueous solution was left for a few days until a blue coloration appeared. An organic solution of 0.1 M tetrabutylammonium perchlorate in 1,2-dichloroethane was prepared. To prepare the water droplet system, an aliquot of the aqueous solution (15 or 30 μL) was added to 5 mL of the organic solution that is in a 10 mL fluorinated ethylene propylene tube. Then, a horn sonicator was used. After this, a cloudy emulsion was obtained, an indication of water droplets suspended in 1,2-dichloroethane. These solutions were used either for dynamic light scattering measurements or for the electrodeposition of IrO_x nanoparticles using chronoamperometry.

The TEM sample was prepared with a reverse tweezer. The solution used was the emulsion of the water solution (30 μL) in 5 mL of the organic solution. The working electrode was a carbon-based TEM grid. The grid was held with the tweezer. After that, the tweezer was connected to the working electrode clamp of the potentiostat for a regular electrochemical experiment.

After the electrodeposition process, the working electrode was submerged in a solution of ethanol for 1 min, followed by

https://doi.org/10.1021/acsnanoscienceau.3c00061
ACS Nanosci. Au 2024, 4, 216−222

submerging the electrode in water for another minute. Then, the electrode was finally submerged in acetone for 1 min. This procedure was performed to ensure that any salt was removed from the surface of the electrode for further characterization.

A sample for XPS analysis was prepared on a glassy carbon electrode. The same water (30 μL) in oil (5 mL) emulsion system was used as our solution. The electrodeposition process was carried out at 1.2 V vs Ag/AgCl. The electrodeposition process was carried out at 1.2 V for 240 s as it was tough to locate the nanoparticles via field emission scanning electron microscope (FESEM) at lower potentials due to low coverage. After the electrodeposition process, the electrode was submerged in ethanol and water to remove salt from the surface of the electrode.

RESULTS AND DISCUSSION

Studying electrochemistry in single nanodroplets has been previously shown to be very helpful in understanding the reactivity of single entities, studying their nucleation and growth properties, understanding the kinetics and thermodynamics of the process, and many more uses.[24−26,34,43,44] Here, we are using a reverse emulsion system (water nanodroplets in an organic phase) to achieve the electrodeposition of IrO_x in anodic conditions by confining the reactions in nanoreactors (i.e., water nanodroplets). Scheme 1 represents our reverse emulsion system, comprising water nanodroplets suspended in a 1,2-dichloroethane phase containing tetrabutylammonium perchlorate salt. The water nanodroplets contained a metal precursor salt (K_3IrCl_6), NaOH, and KCl. With time, the nanodroplets collided with the glassy carbon electrode, and via electrochemical oxidation, we were able to generate IrO_x nanoparticles.

Initially, the K_3IrCl_6 solution did not contain any NaOH in the water phase. However, in this case, IrO_x was not observed on the electrode surface, meaning that IrO_x was not electrodeposited (Figure S1). Therefore, a new strategy needed to be considered, and considering Casella's work, NaOH was added to the water phase.[45] The solution was aged for a few days, and a blue color eventually appeared. The innovative idea behind this is to make the K_3IrCl_6 solution into an iridium chloro-hydroxy complex, which will later be oxidized to IrO_x at anodic potentials.[45]

Before the electrochemical experiments were performed, the partitioning of the metal salt between the water and 1,2-dichloroethane phases should be considered. One of the main aspects of nanodroplet-mediated electrodeposition is that it enables control of the nanoparticle size and morphology by confining the redox reaction inside the aqueous nanodroplet. Therefore, the partitioning of the metal salt between water and 1,2-dichloroethane is undesirable as it limits the ability to control nanoparticle size and may cause background electrodeposition reactions in the continuous phase. To take care of this issue, as a control, colorimetric experiments were performed, which ensured that no appreciable $IrCl_6^{3-}$ was transferred from the water phase into the 1,2-dichloroethane (Figure S2). In the aqueous phase (dark blue color), we have 6 mM potassium hexachloroiridate(III), 20 mM KCl, and 55 mM NaOH. In the organic phase (colorless), 0.1 M tetrabutylammonium perchlorate was added to 1,2-DCE. The solution was vigorously shaken and then kept at rest. It can be observed in Figure S2 that the bottom organic solution stays clear (without any bluish coloration), an indication that the Ir salt does not transfer into the organic phase and that the electrochemical reaction occurs via the nanodroplet (nanoreactor).

Before depositing via amperometry, the oxidation potential of our K_3IrCl_6 solution was determined. This was done utilizing the cyclic voltammetric (CV) technique. Figure 1 shows the CV profile of the K_3IrCl_6 solution (in black) compared to the control, containing no K_3IrCl_6 and having only NaOH and KCl in the water nanodroplets (in red). A clear distinction was seen between the two: for the one containing K_3IrCl_6, anodic peaks were seen at ∼0.6 and 0.85 V vs Ag/AgCl (Figure 1, black line). Our negative control (in red) showed no peaks, helping us to validate the claim that the K_3IrCl_6 solution is getting oxidized at ∼0.6−0.9 V vs Ag/AgCl. A hypothesis of the mechanism of the electrodeposition process was provided by Casella.[45] Figure 1 depicts a clear-cut redox system (Ia/Ib) in the potential region at ∼0.6 and 0.47 V in the CV data, which has been previously assigned in the literature to the Ir(III)/Ir(IV) redox transition.[44] Higher oxidation states of Ir(V) or Ir(VI) have been hypothesized before for peak IIa in the CV.[45,46] However, the current literature is not comprehensive and explicit about the complexity of the iridium system.[45,47]

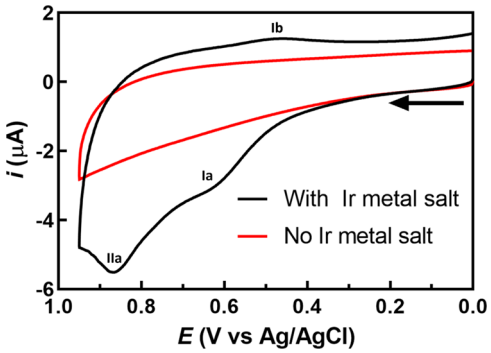

Figure 1. Cyclic voltammogram of an emulsion solution of (a) 6 mM potassium hexachloroiridate(III) with 20 mM KCl and 55 mM NaOH in water nanodroplets suspended in 1,2-dichloroethane with 0.1 M tetrabutylammonium perchlorate and (b) 20 mM KCl with 55 mM NaOH in water nanodroplets suspended in 1,2-dichloroethane with 0.1 M tetrabutylammonium perchlorate. The scan rate was 50 mV/s. To prepare the emulsion, 15 μL of the aqueous phase was added to 5 mL of the 1,2-dichloroethane phase, and then the mixture was sonicated. Polarographic notation was used.

The electrodeposition of IrO_x was performed via amperometry at 1.2 V vs Ag/AgCl for 240 s on a glassy carbon electrode (Figure S3). Amperometry was performed because it enables one to select a potential where IrO_x can be electrodeposited for a selected amount of time. Figure 2 shows the SEM images of the IrO_x deposited nanoparticles (white and gray in color) on the glassy carbon electrode (black in color). IrO_x particles appeared to be globular in shape; some particles were isolated, and some were aggregated.

This result is in good agreement with previously observed IrO_x nanoparticles.[45] The particle's average diameter was 43 nm with a standard deviation of 10 nm. Thus, with the nanodroplet-mediated electrodeposition method, it is shown that it is possible to obtain oxide nanoparticles with a diameter of tens of nanometers by confining the reaction inside the water nanodroplets. Their chemical composition was confirmed with EDX and peaks for iridium and oxygen were

https://doi.org/10.1021/acsnanoscienceau.3c00061
ACS Nanosci. Au 2024, 4, 216−222

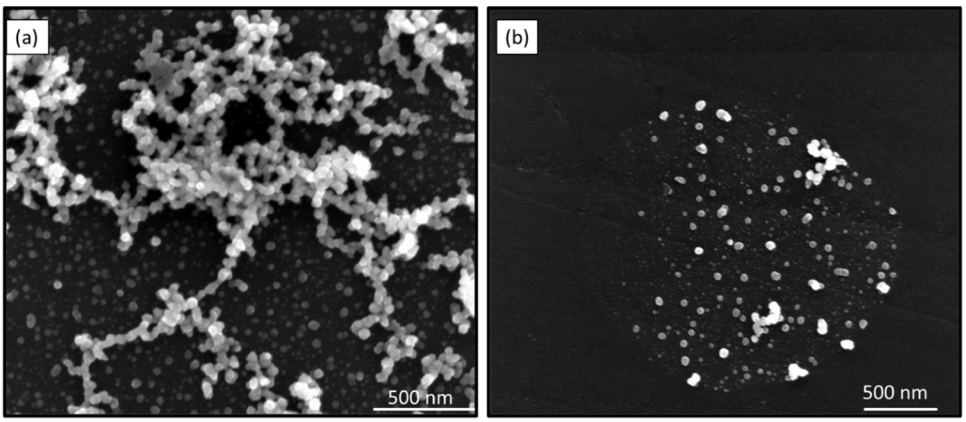

Figure 2. SEM image of IrO_x nanoparticles electrodeposited on the glassy carbon electrode surface. An emulsion was used to generate these nanoparticles. An emulsion of 6 mM potassium hexachloroiridate(III) with 20 mM KCl and 55 mM NaOH in water nanodroplets suspended in 1,2-dichloroethane with 0.1 M tetrabutylammonium perchlorate was used. To prepare the emulsion, 15 μL of the aqueous phase was added to 5 mL of the 1,2-dichloroethane phase and the horn sonicator was used. Parts (a) and (b) represent two different areas of the electrode.

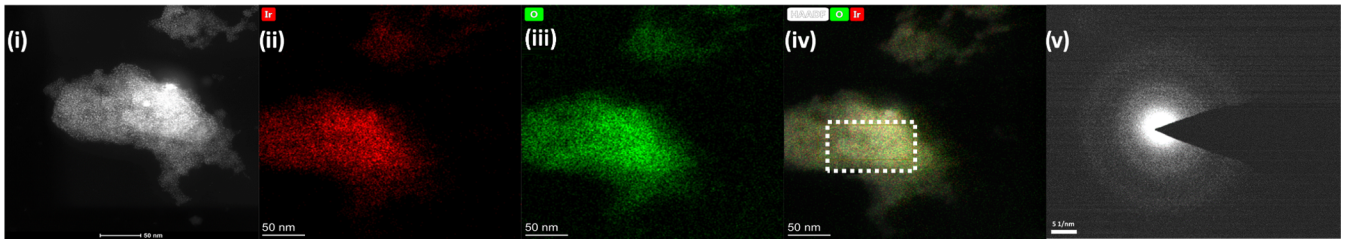

Figure 3. (i) STEM-HAADF image of our IrO_x nanoparticles. (ii) and (iii) represent the EDX mapping of Ir and O, respectively, and (iv) represents an overlay of all Ir and O. The scale bar is 50 nm for (i), (ii), (iii), and (iv). (v) represents the selected area electron diffraction (SAED) of our deposited nanoparticles (scale bar: 5 nm^{-1}).

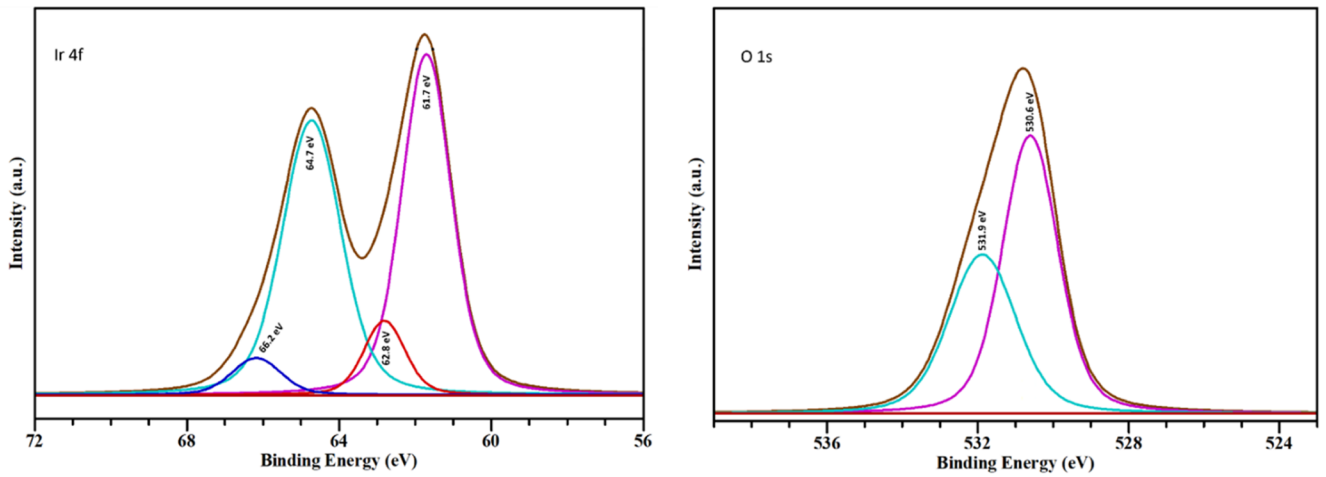

Figure 4. XPS results for the Ir 4f and O 1s region of the IrO_x sample electrodeposited on the glassy carbon electrode.

observed (Figure S4), indicative of the presence of IrO_x nanoparticles.

Additionally, a control was performed with the same water-in-oil emulsion but without applying a potential. The SEM image showed the deposition of K_3IrCl_6 salt, and EDX showed peaks for iridium, oxygen, and chlorine (Figure S5). This is the result of the K_3IrCl_6 solution sticking to the electrode. This implies that the particles observed in Figure 2 are the product of an oxidation reaction of a K_3IrCl_6 solution under anodic potentials.

IrO_x was electrodeposited on a carbon-based TEM grid via amperometry at 1.2 V vs Ag/AgCl. High-angle annular dark-field scanning transmission electron microscopy (HAADF-STEM) was performed at 200 kV on the electrodeposited IrO_x nanoparticle. Figure 3 shows a HAADF-STEM image of an IrO_x nanoparticle. EDX mapping was done, showing the presence of iridium (Figure 3,ii), oxygen (Figure 3,iii), and the overlay of iridium and oxygen (Figure 3,iv). EDX spectra obtained from the dashed white box in Figure 3,iv show the peaks of iridium and oxygen (Figure S6). The nanoparticle did not distort even at 200 kV. Moreover, Figure 3,v shows selected area electron diffraction (SAED) performed on our electrodeposited sample on the TEM grid. SAED shows clear rings without any bright spots, indicating that our deposited

https://doi.org/10.1021/acsnanoscienceau.3c00061
ACS Nanosci. Au 2024, 4, 216−222

sample is amorphous in nature. This goes on to hint at the absence of our precursor salt complex and the presence of our oxidized species. Multiple SAED were run on TEM images with different shapes and sizes (Figure S11).

XPS Characterization

To carry out the measurement for XPS, IrO_x was electrodeposited on a glassy carbon electrode at 1.2 V vs Ag/AgCl. In this study, the absence of the Cl 2p signal (Figure S7) indicates that the electrode surface contains only iridium and oxygen species.[43] This is well aligned with our previous discussion, where we talked about the oxidation of the chloro-hydroxy complex to iridium oxide. XPS analysis in Figure 4 revealed distinct peaks at 61.7 ± 0.2 and 64.7 ± 0.2 eV, corresponding to Ir(III) and Ir(IV), and tentatively assigned peaks at 530.6 ± 0.4 and 531.9 ± 0.4 eV to hydroxide and hydration water in the O 1s signal.[48−51] Furthermore, the O 1s/Ir ($4f_{7/2}$ + $4f_{5/2}$) ratio increased with the decreasing Ir(III)/Ir(IV) ratio, suggesting that Ir(IV) complexes contained more oxygen than the Ir(III) species. These findings provide essential insights into the composition and surface chemistry of iridium species on the electrode, and they are well aligned with previously reported iridium oxide nanoparticles.[43]

Studying Different Parameters on the Electrodeposition of IrO_x

We analyzed the IrO_x electrodeposition at two different volumes of the aqueous phase, 30 and 15 μL, as shown in Figure S8b,c, respectively. A stark contrast was seen between the two in terms of the nanodroplet size and the coverage of the IrO_x deposition on the electrode. The nanodroplet size was measured by using dynamic light scattering (DLS) (Figure S8a). At 30 μL, nanodroplets of a diameter of around 720 nm were observed, and IrO_x deposition was seen throughout the electrode (Figure S8b). At 15 μL, 490 nm diameter nanodroplets were obtained, and fewer IrO_x particles were seen around the surface of the electrode (Figure S8c). These results show that nanodroplet size and coverage of particles on the electrode depend on the amount of the aqueous phase added to the organic solution. By adding small volumes, smaller nanodroplets are observed, and fewer particles are seen on the electrode surface. On the other hand, when larger volumes are added, we see bigger nanodroplets and a higher number of particles on the surface of the electrode. Figure S8a also has interesting areas of dark contrast in a field of IrO_x nanoparticles. We have previously assigned these "inclusions" to pockets of 1,2-dichloroethane when neighboring nanodroplets fuse.[52]

We studied the effect of the surfactant, 0.01% v/v Span 80, which was added in the 1,2-dichloroethane phase. Span 80 has been previously reported as a stabilizing agent for reverse emulsion systems (water-in-oil systems).[53] After adding Span 80 in the 1,2- dichloroethane phase, no appreciable deposition was observed even at 1.2 V versus Ag/AgCl (Figure S8d,e). It has been reported before how a surfactant forms a layer between the electrode and the solution phase and blocks the area available for the reaction.[54]

To see the effect of precursor salt on the electrodeposited nanoparticle, our group previously reported an increase in the size of electrodeposited Pt with increasing precursor concentration.[30] We also performed an experiment by taking 12 mM (Figure S9) of the Ir precursor salt compared to the 6 mM taken before and followed the same procedure as listed previously to get the electrodeposited IrO_x nanoparticles. The particle size was around 115 ± 12 nm, quite bigger than the previously reported 43 ± 10 nm for 6 mM.

Au ultramicroelectrode (UME) was tried as a substrate to deposit IrO_x. We did see collision peaks (Figure S10), which signify the electrolysis of our complex and indicate the deposition of IrO_x nanoparticles. Thus, ultramicroelectrodes (UMEs) may be employed to understand species diffusion, nucleation, and growth kinetics of IrO_x nanoparticles.[44] These remain a part of our future inquiry.

CONCLUSIONS

Nanodroplet-mediated electrodeposition has been shown once again to be a powerful technique to generate nanoparticles. Here, we present for the first time the electrodeposition of metal oxide nanoparticles under anodic conditions with water nanodroplets. It was shown that IrO_x nanoparticles were electrodeposited at anodic potential without the need to perform cycling with cyclic voltammetry or use multiple potential steps with chronoamperometry. The electrodeposited IrO_x nanoparticles were characterized using FESEM, EDX, STEM, SAED, and XPS. The anodic electrodeposition of IrO_x via aqueous nanodroplets has opened up a new avenue in the field of nanodroplet-mediated electrodeposition. This should lead to the further synthesis of other metal oxides at anodic potentials via aqueous nanodroplets. This new electrosynthetic method of using water nanodroplets to generate metal oxide nanoparticles at anodic conditions goes on to show the versatility of the nanodroplet-mediated electrodeposition technique.

ASSOCIATED CONTENT

Supporting Information

The Supporting Information is available free of charge at https://pubs.acs.org/doi/10.1021/acsnanoscienceau.3c00061.

IrO_x electrodeposition chronoamperogram; SEM and EDX characterization of electrodeposited particles; TEM and SAED of electrodeposited particles; XPS data; control experiments without NaOH, without applied potential, and to see partitioning of metal salt; and effect of the nanodroplet size, surfactant, concentration of precursor salt, and different substrates on electrodeposited IrO_x (PDF)

AUTHOR INFORMATION

Corresponding Author

Jeffrey E. Dick − *Department of Chemistry, Purdue University, West Lafayette, Indiana 47907, United States; Elmore Family School of Electrical and Computer Engineering, Purdue University, West Lafayette, Indiana 47907, United States;* orcid.org/0000-0002-4538-9705; Email: jdick@purdue.edu

Authors

Saptarshi Paul − *Department of Chemistry, Purdue University, West Lafayette, Indiana 47907, United States*

Joshua Reyes-Morales − *Department of Chemistry, Purdue University, West Lafayette, Indiana 47907, United States*

Kingshuk Roy − *Department of Chemistry, Purdue University, West Lafayette, Indiana 47907, United States*

Complete contact information is available at: https://pubs.acs.org/10.1021/acsnanoscienceau.3c00061

https://doi.org/10.1021/acsnanoscienceau.3c00061
ACS Nanosci. Au 2024, 4, 216−222

Author Contributions

†S.P. and J.R.-M. contributed equally. All authors have approved the final version of the manuscript. CRediT: **Saptarshi Paul** data curation, formal analysis; **Joshua Reyes-Morales** data curation; **Kingshuk Roy** conceptualization; **Jeffrey E. Dick** supervision.

Notes

The authors declare no competing financial interest.

■ ACKNOWLEDGMENTS

The authors would like to acknowledge the use of facilities within the Purdue Electron Microscopy Center. Facility RRID SCR_022687. XPS data were obtained at the Surface Analysis Facility of the Birck Nanotechnology Center at Purdue University. The authors acknowledge the support from the National Science Foundation CAREER under grant number CHE-2045672 and would also like to acknowledge Ashutosh Rana of Purdue University for helping with the schematic figure.

■ REFERENCES

(1) Mohanty, U. S. Electrodeposition: a versatile and inexpensive tool for the synthesis of nanoparticles, nanorods, nanowires, and nanoclusters of metals. *J. Appl. Electrochem.* **2011**, *41*, 257−270.
(2) Jayakrishnan, D. S. Electrodeposition: the Versatile Technique for Nanomaterials. In *Corrosion Protection and Control using Nanomaterials*; Elsevier, 2012; pp 86−125.
(3) Winand, R. Electrodeposition of metals and alloys—new results and perspectives. *Electrochim. Acta* **1994**, *39* (8−9), 1091−1105.
(4) Simka, W.; Puszczyk, D.; Nawrat, G. Electrodeposition of metals from non-aqueous solutions. *Electrochim. Acta* **2009**, *54* (23), 5307−5319.
(5) Abbott, A. P.; McKenzie, K. J. Application of ionic liquids to the electrodeposition of metals. *Phys. Chem. Chem. Phys.* **2006**, *8* (37), 4265−4279.
(6) Endres, F. Ionic liquids: solvents for the electrodeposition of metals and semiconductors. *ChemPhysChem* **2002**, *3* (2), 144−154.
(7) Kenney, M. J.; Huang, J. E.; Zhu, Y.; Meng, Y.; Xu, M.; Zhu, G.; Hung, W.-H.; Kuang, Y.; Lin, M.; Sun, X.; et al. An electrodeposition approach to metal/metal oxide heterostructures for active hydrogen evolution catalysts in near-neutral electrolytes. *Nano Res.* **2019**, *12*, 1431−1435.
(8) Switzer, J. A.; Liu, R.; Bohannan, E. W.; Ernst, F. Epitaxial electrodeposition of a crystalline metal oxide onto single-crystalline silicon. *J. Phys. Chem. B* **2002**, *106* (48), 12369−12372.
(9) Yar, A.; Krishnan, S. G.; Dennis, J. O.; Yasin, A.; Khalid, M.; Yang, C.-C.; Jose, R. Metal oxide nanotubes via electrodeposition for battery-electrochemical capacitor hybrid device. *Synth. Met.* **2022**, *284*, No. 116991.
(10) Monk, P. M. S.; Chester, S. L. Electro-deposition of films of electrochromic tungsten oxide containing additional metal oxides. *Electrochim. Acta* **1993**, *38* (11), 1521−1526.
(11) Brenner, A. *Electrodeposition of Alloys: Principles and Practice*; Elsevier, 2013.
(12) Gu, Y.; Liu, J.; Qu, S.; Deng, Y.; Han, X.; Hu, W.; Zhong, C. Electrodeposition of alloys and compounds from high-temperature molten salts. *J. Alloys Compd.* **2017**, *690*, 228−238.
(13) Zangari, G. Electrodeposition of alloys and compounds in the era of microelectronics and energy conversion technology. *Coatings* **2015**, *5* (2), 195−218.
(14) Schley, N. D.; Blakemore, J. D.; Subbaiyan, N. K.; Incarvito, C. D.; D'Souza, F.; Crabtree, R. H.; Brudvig, G. W. Distinguishing homogeneous from heterogeneous catalysis in electrode-driven water oxidation with molecular iridium complexes. *J. Am. Chem. Soc.* **2011**, *133* (27), 10473−10481.
(15) Switzer, J. A.; Kothari, H. M.; Poizot, P.; Nakanishi, S.; Bohannan, E. W. Enantiospecific electrodeposition of a chiral catalyst. *Nature* **2003**, *425* (6957), 490−493.
(16) Egetenmeyer, A.; Radev, I.; Durneata, D.; Baumgärtner, M.; Peinecke, V.; Natter, H.; Hempelmann, R. Pulse electrodeposited cathode catalyst layers for PEM fuel cells. *Int. J. Hydrogen Energy* **2017**, *42* (19), 13649−13660.
(17) Ma, X.; Liu, Z.; Chen, H. Facile and scalable electrodeposition of copper current collectors for high-performance Li-metal batteries. *Nano Energy* **2019**, *59*, 500−507.
(18) Popov, G.; Mattinen, M.; Kemell, M. L.; Ritala, M.; Leskelä, M. Scalable route to the fabrication of CH3NH3PbI3 perovskite thin films by electrodeposition and vapor conversion. *ACS Omega* **2016**, *1* (6), 1296−1306.
(19) Chen, H.; Wei, Z.; Zheng, X.; Yang, S. A scalable electrodeposition route to the low-cost, versatile and controllable fabrication of perovskite solar cells. *Nano Energy* **2015**, *15*, 216−226.
(20) Fierro, S.; Kapałka, A.; Comninellis, C. Electrochemical comparison between IrO2 prepared by thermal treatment of iridium metal and IrO2 prepared by thermal decomposition of H2IrCl6 solution. *Electrochem. Commun.* **2010**, *12* (1), 172−174.
(21) Nishio, K.; Watanabe, Y.; Tsuchiya, T. Preparation and properties of electrochromic iridium oxide thin film by sol-gel process. *Thin Solid Films* **1999**, *350* (1), 96−100.
(22) Roy, E.; Fricoteaux, P.; Yu-Zhang, K. Electrochemical synthesis of antimony nanowires and analysis of diffusion layers. *J. Nanosci. Nanotechnol.* **2001**, *1* (3), 323−329.
(23) Schiavi, P. G.; Altimari, P.; Zanoni, R.; Pagnanelli, F. Morphology-controlled synthesis of cobalt nanostructures by facile electrodeposition: transition from hexagonal nanoplatelets to nanoflakes. *Electrochim. Acta* **2016**, *220*, 405−416.
(24) Reyes-Morales, J.; Dick, J. E. Electrochemical-Shock Synthesis of Nanoparticles from Sub-femtoliter Nanodroplets. *Acc. Chem. Res.* **2023**, *56* (10), 1178−1189.
(25) Reyes-Morales, J.; Moazeb, M.; Colón-Quintana, G. S.; Dick, J. E. The electrodeposition of gold nanoparticles from aqueous nanodroplets. *Chem. Commun.* **2022**, *58* (76), 10663.
(26) Reyes-Morales, J.; Vanderkwaak, B. T.; Dick, J. E. Enabling practical nanoparticle electrodeposition from aqueous nanodroplets. *Nanoscale* **2022**, *14* (7), 2750.
(27) Pendergast, A. D.; Glasscott, M. W.; Renault, C.; Dick, J. E. One-step electrodeposition of ligand-free PdPt alloy nanoparticles from water droplets: Controlling size, coverage, and elemental stoichiometry. *Electrochem. Commun.* **2019**, *98*, 1−5.
(28) Glasscott, M. W.; Pendergast, A. D.; Dick, J. E. A Universal Platform for the Electrodeposition of Ligand-Free Metal Nanoparticles from a Water-in-Oil Emulsion System. *ACS Appl. Nano Mater.* **2018**, *1* (10), 5702.
(29) Tarolla, N. E.; Voci, S.; Reyes-Morales, J.; Pendergast, A. D.; Dick, J. E. Electrodeposition of ligand-free copper nanoparticles from aqueous nanodroplets. *J. Mater. Chem. A* **2021**, *9* (35), 20048−20057.
(30) Glasscott, M. W.; Pendergast, A. D.; Dick, J. E. A Universal Platform for the Electrodeposition of Ligand-Free Metal Nanoparticles from a Water-in-Oil Emulsion System. *ACS Appl. Nano Mater.* **2018**, *1* (10), 5702−5711.
(31) Glasscott, M. W.; Pendergast, A. D.; Goines, S.; Bishop, A. R.; Hoang, A. T.; Renault, C.; Dick, J. E. Electrosynthesis of high-entropy metallic glass nanoparticles for designer, multi-functional electrocatalysis. *Nat. Commun.* **2019**, *10* (1), No. 2650.
(32) Percival, S. J.; Lu, P.; Lowry, D. R.; Nenoff, T. M. Electrodeposition of Complex High Entropy Oxides via Water Droplet Formation and Conversion to Crystalline Alloy Nanoparticles. *Langmuir* **2022**, *38* (5), 1923−1928.
(33) Jeun, Y. E.; Baek, B.; Lee, M. W.; Ahn, H. S. Surfactant-free electrochemical synthesis of metallic nanoparticles via stochastic collisions of aqueous nanodroplet reactors. *Chem. Commun.* **2018**, *54* (72), 10052−10055.
(34) Glasscott, M. W.; Pendergast, A. D.; Choudhury, M. H.; Dick, J. E. Advanced Characterization Techniques for Evaluating Porosity,

Nanopore Tortuosity, and Electrical Connectivity at the Single-Nanoparticle Level. *ACS Appl. Nano Mater.* **2019**, *2* (2), 819−830.
(35) Zhuang, L.; Xu, F.; Wang, K.; Li, J.; Liang, C.; Zhou, W.; Xu, Z.; Shao, Z.; Zhu, Z. Porous Structure Engineering of Iridium Oxide Nanoclusters on Atomic Scale for Efficient pH-Universal Overall Water Splitting. *Small* **2021**, *17* (20), No. 2100121.
(36) Lattach, Y.; Rivera, J. F.; Bamine, T.; Deronzier, A.; Moutet, J.-C. Iridium oxide−polymer nanocomposite electrode materials for water oxidation. *ACS Appl. Mater. Interfaces* **2014**, *6* (15), 12852−12859.
(37) El Khakani, M. A.; Chaker, M.; Gat, E. Pulsed laser deposition of highly conductive iridium oxide thin films. *Appl. Phys. Lett.* **1996**, *69* (14), 2027−2029.
(38) Cherevko, S.; Reier, T.; Zeradjanin, A. R.; Pawolek, Z.; Strasser, P.; Mayrhofer, K. J. J. Stability of nanostructured iridium oxide electrocatalysts during oxygen evolution reaction in acidic environment. *Electrochem. Commun.* **2014**, *48*, 81−85.
(39) Jang, H.; Lee, J. Iridium oxide fabrication and application: A review. *J. Energy Chem.* **2020**, *46*, 152−172.
(40) Beknalkar, S. A.; Teli, A. M.; Harale, N. S.; Patil, D. S.; Pawar, S. A.; Shin, J. C.; Patil, P. S. Fabrication of high energy density supercapacitor device based on hollow iridium oxide nanofibers by single nozzle electrospinning. *Appl. Surf. Sci.* **2021**, *546*, No. 149102.
(41) Wang, M.; Yao, S.; Madou, M. A long-term stable iridium oxide pH electrode. *Sens. Actuators, B* **2002**, *81* (2−3), 313−315.
(42) Meyer, R. D.; Cogan, S. F.; Nguyen, T. H.; Rauh, R. D. Electrodeposited iridium oxide for neural stimulation and recording electrodes. *IEEE Trans. Neural Syst. Rehabil. Eng.* **2001**, *9* (1), 2−11.
(43) Glasscott, M. W.; Dick, J. E. Fine-Tuning Porosity and Time-Resolved Observation of the Nucleation and Growth of Single Platinum Nanoparticles. *ACS Nano* **2019**, *13* (4), 4572−4581.
(44) Glasscott, M. W.; Hill, C. M.; Dick, J. E. Quantifying Growth Kinetics of Single Nanoparticles in Sub-Femtoliter Reactors. *J. Phys. Chem. C* **2020**, *124* (26), 14380−14389.
(45) Casella, I. G.; Contursi, M.; Toniolo, R. Anodic electrodeposition of iridium oxide particles on glassy carbon surfaces and their electrochemical/SEM/XPS characterization. *J. Electroanal. Chem.* **2015**, *736*, 147−152.
(46) Arroyo-Currás, N.; Bard, A. J. Iridium oxidation as observed by surface interrogation scanning electrochemical microscopy. *J. Phys. Chem. C* **2015**, *119* (15), 8147−8154.
(47) Suzuki, H.; Arakawa, H.; Sasaki, S.; Karube, I. Micromachined Severinghaus-type carbon dioxide electrode. *Anal. Chem.* **1999**, *71* (9), 1737−1743.
(48) Pickup, P. G.; Birss, V. I. The influence of the aqueous growth medium on the growth rate, composition, and structure of hydrous iridium oxide films. *J. Electrochem. Soc.* **1988**, *135* (1), 126.
(49) Da Silva, L.; Alves, V.; De Castro, S.; Boodts, J. XPS study of the state of iridium, platinum, titanium and oxygen in thermally formed IrO2+ TiO2+ PtOX films. *Colloids Surf., A* **2000**, *170* (2−3), 119−126.
(50) Kodintsev, I. M.; Trasatti, S.; Rubel, M.; Wieckowski, A.; Kaufher, N. X-ray photoelectron spectroscopy and electrochemical surface characterization of iridium (IV) oxide+ ruthenium (IV) oxide electrodes. *Langmuir* **1992**, *8* (1), 283−290.
(51) Le Vot, S.; Roué, L.; Bélanger, D. Electrodeposition of iridium onto glassy carbon and platinum electrodes. *Electrochim. Acta* **2012**, *59*, 49−56.
(52) Voci, S.; Clarke, T. B.; Dick, J. E. Abiotic microcompartments form when neighbouring droplets fuse: an electrochemiluminescence investigation. *Chem. Sci.* **2023**, *14* (9), 2336−2341.
(53) Fu, Z.; Liu, M.; Xu, J.; Wang, Q.; Fan, Z. Stabilization of water-in-octane nano-emulsion. Part I: Stabilized by mixed surfactant systems. *Fuel* **2010**, *89* (10), 2838−2843.
(54) Tsionsky, M.; Bard, A. J.; Mirkin, M. V. Long-Range Electron Transfer through a Lipid Monolayer at the Liquid/Liquid Interface. *J. Am. Chem. Soc.* **1997**, *119* (44), 10785−10792.

https://doi.org/10.1021/acsnanoscienceau.3c00061
ACS Nanosci. Au 2024, 4, 216−222